



A High Luminosity, High Energy Electron-Ion-Collider

*A New Experimental Quest to Study the Glue
That Binds Us All*

The Electron Ion Collider Working Group

April 24, 2007

Recommendations

Unanimous recommendation of the Quantum Chromodynamics Town Meeting, at Rutgers University, New Jersey, January, 2007

A high luminosity Electron Ion Collider (EIC) is the highest priority of the QCD community for new construction after the Jlab12 GeV and RHIC II upgrades. EIC will address compelling physics questions essential for understanding the fundamental structure of matter:

- *Precision imaging of the sea-quark and gluons to determine the spin, flavor and spatial structure of the nucleon*
- *Definitive study of the universal nature of strong gluon fields in nuclei*

The collider and the detector designs must be developed expeditiously.

DOE Office of Science Strategic Plan, February 2004

The eRHIC is identified as the far term priority facility to explore the structure of nuclear matter.

The Nuclear Physics Scientific Horizon: Projects for the Next Twenty Years Report of the Ad-hoc Facilities Subcommittee of NSAC, March 2003

We find that an electron ion collider is absolutely central to the U.S. Science.

Long Range Plan for Nuclear Science by NSAC, 2002

The electron ion collider is an extremely exciting initiative for the future of nuclear science in the U.S.

The EIC Working Group

(April 2007)

¹⁷C. Aidala, ²⁸E. Aschenauer, ¹⁰J. Annand, ¹J. Arrington, ²⁶R. Averbeck, ³M. Baker, ²⁶K. Boyle, ²⁸W. Brooks, ²⁸A. Bruell, ¹⁹A. Caldwell, ²⁸J.P. Chen, ²R. Choudhury, ¹⁰E. Christy, ⁸B. Cole, ⁴D. De Florian, ³R. Debbe, ^{26,24-1}A. Deshpande**, ¹⁸K. Dow, ²⁶A. Drees, ³J. Dunlop, ²D. Dutta, ⁷F. Ellinghaus, ²⁸R. Ent, ¹⁸R. Fatemi, ¹⁸W. Franklin, ²⁸D. Gaskell, ¹⁶G. Garvey, ^{12,24-1}M. Grosse-Perdekamp, ¹K. Hafidi, ¹⁸D. Hasell, ²⁶T. Hemmick, ¹R. Holt, ⁸E. Hughes, ²²C. Hyde-Wright, ⁵G. Igo, ¹⁴K. Imai, ¹⁰D. Ireland, ²⁶B. Jacak, ¹⁵P. Jacobs, ²⁸M. Jones, ¹⁰R. Kaiser, ¹⁷D. Kawall, ¹¹C. Keppel, ⁷E. Kinney, ¹⁸M. Kohl, ⁹H. Kowalski, ¹⁷K. Kumar, ²V. Kumar, ²¹G. Kyle, ¹³J. Lajoie, ¹⁶M. Leitch, ²⁷A. Levy, ²⁷J. Lichtenstadt, ¹⁰K. Livingstone, ²⁰W. Lorenzon, ¹⁴5. Matis, ¹²N. Makins, ⁶G. Mallot, ¹⁸M. Miller, ¹⁸R. Milner**, ²A. Mohanty, ³D. Morrison, ²⁶Y. Ning, ¹⁵G. Odyniec, ¹³C. Ogilvie, ²L. Pant, ²⁶V. Pantuyev, ²¹S. Pate, ²⁶P. Paul, ¹²J.-C. Peng, ¹⁸R. Redwine, ¹P. Reimer, ¹⁵H.-G. Ritter, ¹⁰G. Rosner, ²⁵A. Sandacz, ⁷J. Seele, ¹²R. Seidl, ¹⁰B. Seitz, ²P. Shukla, ¹⁵E. Sichtermann, ¹⁸F. Simon, ³P. Sorensen, ³P. Steinberg, ²⁴M. Stratmann, ²²M. Strikman, ¹⁸B. Surrow, ¹⁸E. Tsentalovich, ¹¹V. Tvaskis, ³T. Ullrich, ³R. Venugopalan, ³W. Vogelsang, ²⁸C. Weiss, ¹⁵H. Wieman, ¹⁵N. Xu, ³Z. Xu, ⁸W. Zajc.

¹Argonne National Laboratory, Argonne, IL; ²Bhabha Atomic Research Centre, Mumbai, India; ³Brookhaven National Laboratory, Upton, NY; ⁴University of Buenos Aires, Argentina; ⁵University of California, Los Angeles, CA; ⁶CERN, Geneva, Switzerland; ⁷University of Colorado, Boulder, CO; ⁸Columbia University, New York, NY; ⁹DESY, Hamburg, Germany; ¹⁰University of Glasgow, Scotland, United Kingdom; ¹¹Hampton University, Hampton, VA; ¹²University of Illinois, Urbana-Champaign, IL; ¹³Iowa State University, Ames, IA; ¹⁴University of Kyoto, Japan; ¹⁵Lawrence Berkeley National Laboratory, Berkeley, CA; ¹⁶Los Alamos National Laboratory, Los Alamos, NM; ¹⁷University of Massachusetts, Amherst, MA; ¹⁸MIT, Cambridge, MA; ¹⁹Max Planck Institut für Physik, Munich, Germany; ²⁰University of Michigan Ann Arbor, MI; ²¹New Mexico State University, Las Cruces, NM; ²²Old Dominion University, Norfolk, VA; ²³Penn State University, PA; ²⁴RIKEN, Wako, Japan; ²⁴⁻¹RIKEN-BNL Research Center, BNL, Upton, NY; ²⁵Soltan Institute for Nuclear Studies, Warsaw, Poland; ²⁶SUNY, Stony Brook, NY; ²⁷Tel Aviv University, Israel; ²⁸Thomas Jefferson National Accelerator Facility, Newport News, VA

** EIC WG Contact/Spokespeople: Abhay.Deshpande@StonyBrook.Edu & Milner@Mit.Edu

Table of Contents

1	Perspective.....	4
2	Scientific Highlights.....	8
2.1	<i>Precision Study of the of gluon distribution in the Nucleon.....</i>	8
2.2	<i>The Nucleon Spin Structure.....</i>	9
2.2.1	Precision studies of u,d, and s quark & anti-quark polarization.....	10
2.2.2	Precision determination of the spin dependent gluon distribution at small-x.....	13
2.2.3	Generalized parton distributions & hard exclusive processes	16
2.2.4	Transverse spin and transverse momentum dependent parton distributions.....	19
2.2.5	Study of Hadronization.....	21
2.2.6	Spin Structure of the Photon.....	21
2.3	<i>What are the properties of high density partonic matter?.....</i>	22
2.3.1	Momentum distribution of quarks and gluons in nuclei.....	24
2.3.2	Space-time distribution of gluons and quarks.....	25
2.3.3	Scattering and hadronization of fast probes in an extended gluonic medium.....	27
2.3.4	Role of color neutral degrees (Pomerons) of freedom in scattering of nuclei.....	28
2.3.5	Complementarity of pA and eA studies at low x.....	28
3	The Electron Ion Collider – Realization.....	29
3.1	<i>The EIC Accelerator Design.....</i>	29
3.2	<i>The EIC Detector Design.....</i>	31
4	Conclusion.....	32
	References.....	33

I Perspective

Quantum Chromodynamics (QCD) has been established for three decades now as the theory of the strong interaction, quantitatively validated, with a remarkable precision, by a host of experiments at high energies. QCD differs markedly from QED in that the running coupling constant becomes large at hadronic length scales and in that gluons also interact with gluons. Unlike any other many-body system, the individual quark and gluon constituents making up nucleons and atomic nuclei cannot be removed from the system and examined in isolation. One of the most profound discoveries in physics has been that the mass of atomic nuclei arises predominantly from the binding energy due to gluon interaction, with a large ‘sea’ of gluons constantly fluctuating into quark-anti-quark pairs. This picture of the nucleon as being composed of an infinite number of highly relativistic and nearly mass-less spin- $1/2$ -quarks exchanging spin-1 gluons is completely different from previous physical theories describing the structure of matter, *e.g.* atomic electrons or nucleon models of nuclei, where the binding energy is typically much smaller than the masses of the constituents. The study of the ‘sea’ in the nucleon and atomic nuclei in terms of the constituent gluons and quarks of QCD is a major frontier in nuclear physics, and one essential to obtaining a fundamental understanding of the mass of the visible matter in the universe. Simple questions related to the proton’s structure, such as how does the proton’s spin $1/2$ originate from the dynamics of the quarks and gluons, demand new accelerators with highly-polarized beams at high energies.

At high energies, phases of quark-gluon matter allowed within QCD can be studied directly, and the study of the QCD phase diagram has evolved into a major thrust of nuclear physics at present at RHIC and soon beginning at the LHC. Experiments at RHIC using relativistic heavy ion beams have discovered a new hot, dense matter with the properties of a perfect fluid. The experiments are also consistent with the presence of maximally saturated gluon field strengths in the nuclear wave-functions. As new phenomena in the QCD phase diagram are uncovered and explored, it is clear that measurements of the gluon distributions in heavy nuclei as well as the energy loss of fast quarks and gluons through nuclei will be essential for a rigorous and consistent understanding. Definitive data can only be obtained with a high energy lepton beam.

The future research program into the fundamental quark and gluon structure of matter will focus on three essential questions (adapted from [1]):

- What are the properties of the glue that binds matter into strongly interacting particles?
- What is the quark and gluon structure of the proton?
- What are the properties of high-density quark-gluon matter?

A sustained effort worldwide to determine the optimal experimental approach to address the above questions has resulted in the identification of a high luminosity, high-energy electron-ion-collider (EIC) as the ideal accelerator [2-5]. In this document, we present a high level overview of the scientific case and the machine design for EIC in the context of the 2007 Long Range Planning exercise (for more detailed information on the EIC, see <http://www.bnl.gov/eic>). EIC can provide definitive answers to the above questions and allow a fundamental understanding of the glue which binds us all. EIC will be complementary to the 12 GeV upgrade planned at Jefferson Lab which will focus on the study of the valence quark region.

Gluon distributions have been indirectly measured, through the explicit relationships in QCD between the glue and the ‘sea’ quarks, using high energy deep inelastic (DIS) lepton scattering at HERA [6]. DIS is the unique process, which provides images of the structure of the proton, neutron or nucleus as a function of the quark or gluon momentum fraction (x) at a specific spatial resolution (Q^2). These images are displayed as structure functions and are interpreted rigorously in QCD. Lattice QCD can provide *ab initio* QCD calculations of the moments of the structure functions.

The results from HERA have taught us that gluons dominate at low x , but we know little about the dynamics or properties of this glue: does the strength of this gluon field reach a maximum value and if so what happens in this region of strong field; how do these gluons contribute to the proton and neutron spin? And what is their impact on the transverse dynamics, binding and position distributions of quarks in the proton? These questions cannot be addressed without dramatically increasing the luminosity and kinematic range available to deep-inelastic scattering experiments. Hence, the next generation lepton scattering facility to study the quark and gluon substructure of nucleons (both proton and neutron) and nuclei needs to have the following characteristics:

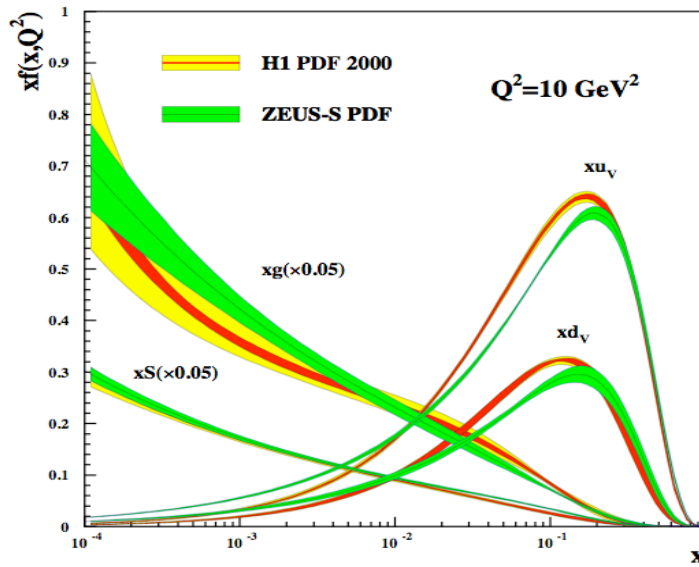


Figure 1. Quark and gluon distributions (valence quark $u_V(x)$, $d_V(x)$; sea quark $S(x)$; gluon $g(x)$) at $Q^2 = 10 \text{ GeV}^2$ as determined at HERA by the H1 and ZEUS experiments [6]. Note the dominance of the gluon and sea quark distributions below $x \sim 0.1$.

- A high energy, high luminosity electron/positron-ion collider with a luminosity of at least $10^{33} \text{ cm}^{-2} \text{ s}^{-1}$ and center-of-mass energies with a range from 20 to 100 GeV. A significant center-of-mass energy range is demanded to effectively use the evolution equations of QCD. Both positron and electron beams are desirable. The reference accelerator design assumes 5-10 GeV electron beams colliding with 25-250 GeV/c proton beams. In a fixed-target configuration, this corresponds to a lepton beam energy of several TeV. The time integrated luminosity determines the final statistical precision in an experiment. The HERA collider has delivered approximately 0.5 fb^{-1} , over about a decade. Hence, with an at least 100 times greater luminosity at EIC, it is reasonable to expect an integrated luminosity in excess of 50 fb^{-1} .
- Polarized ($\sim 70\%$) electron, positron, proton and effective neutron beams. Both polarized nucleon beams are required to comprehensively study the spin structure of the nucleon, one of the central goals of hadron physics. In particular, this will allow a precision test of the Bjorken Sum Rule.
- Nuclear beams from deuterium to uranium: A large range of nuclear beams is required to study the A dependence of nuclear observables. In particular,

universal features of saturated gluon distributions are more accessible experimentally with larger nuclear size.

- A suite of detectors: A central detector to measure DIS processes, both inclusive and with electro-produced hadrons, is essential. In addition, a number of special purpose detectors have been identified to measure specific processes, requiring complete nuclear final state detection.

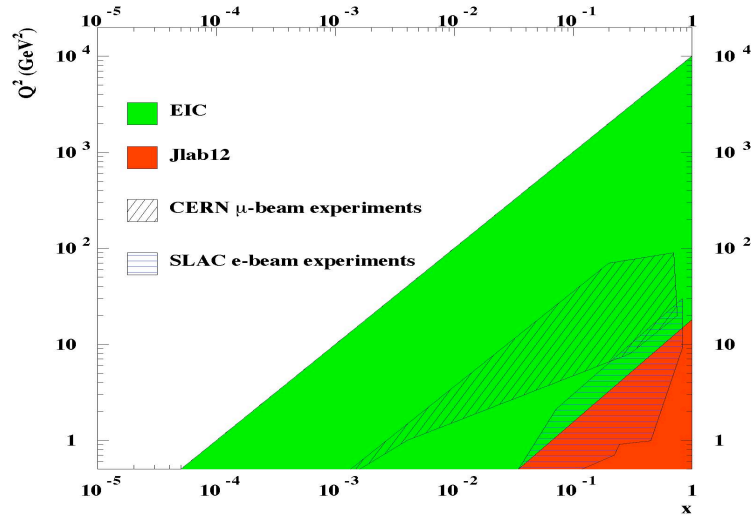


Figure 2. The EIC Q^2 vs. x kinematic plane for a 10 GeV electron beam colliding with a 250 GeV proton beam. The four orders of magnitude reach in x and Q^2 for both polarized nucleon and nuclear beams will explore completely new aspects of hadron structure. EIC is completely complementary to the 12 GeV JLab capability, which studies the valence quark region at much higher luminosity.

EIC is the accelerator facility to explore QCD well beyond any existing frontiers, to allow for unprecedented studies of both the polarization of the glue in the nucleon and the role of quarks and gluons in nuclei. Understanding the physics of glue in detail will have direct and immediate consequences to the understanding of QCD in extreme conditions, and bring fundamental insight to the recent discoveries at RHIC, and to the explorations at much higher energies at LHC.

The science case for EIC was favorably reviewed in the U.S. 2001 Nuclear Physics Long Range Plan, with strong endorsement for R&D. NSAC in March 2003

declared that EIC science was ‘absolutely central to the future of Nuclear Physics.’ eRHIC was identified in November 2003 as a future priority in the DOE Office of Science 20 year plan. EIC is a natural evolution for the U.S. QCD community in that it draws strength from both U.S. nuclear physics flagship facilities, CEBAF and RHIC. EIC will maintain a leadership role for the United States in the study of QCD and will be complementary to the next generation facilities in Europe (LHC@CERN and FAIR@GSI) and Asia (J-PARC).

2 Scientific Highlights

The scientific case for EIC was presented in detail in a white paper at the 2001 Long Range Plan [5], has evolved considerably through succeeding workshops and was most recently described in [6]. EIC directly addresses questions central to the study of QCD. Here a selected few of the highlights are picked to convey the importance and strength of the EIC science case.

2.1 Precision Study of the Gluon Distribution In The Nucleon

Direct study of the glue is best carried out at high energy. Measurements of the structure functions F_2 , the longitudinal structure function, F_L , and of exclusive vector meson production, in the EIC kinematic range would give powerful and distinct information on the gluon distributions. The square of the center of mass energy s , and the four vector energy transfer in a deep inelastic scattering event, Q^2 , are related to the scaling variables Bjorken x and y , through the equation: $s = (Q^2/x)y$. For Q well below the Z boson mass, the unpolarized electron (or positron)-nucleon neutral-current cross section can be written in terms of structure functions as

$$\frac{d^2\sigma^{e\pm N}}{dx dQ^2} = \frac{2\pi\alpha^2}{xQ^4} [(1 + (1 - y)^2) F_2(x, Q^2) - y^2 F_L(x, Q^2)]$$

For small y , the contribution from F_L is negligible, and the cross section effectively yields a direct measurement of F_2 . The evolution of F_2 with Q^2 gives direct sensitivity to the gluon density. At leading order and small values of x , one has:

$$\frac{\partial F_2}{\partial \log Q^2} \propto xg(x, Q^2)$$

This relationship is at the heart of current extractions of the gluon distribution. Analyses of F_2 at HERA have established the rapid rise of the gluon distribution at small x , when $Q \gg 1$ GeV, as shown in Fig.1. The situation at lower Q^2 and small x ,

on the other hand, has remained much less understood. The Q^2 -evolution is ultimately expected to fail here. A telltale sign of this is that the gluon densities extracted at small Q^2 are “valence-like” in almost all next-to-leading order pQCD fits to the data and even become negative in some of them [7]. Other approaches have the promise to yield a description of the relevant physics and lead to new insights into QCD. Among these are, techniques to re-sum all higher order terms [8] or dipole and saturation models [9]. The structure function F_L turns out to be a particularly powerful observable for exploring the physics of this kinematic regime and to conclusively distinguish between the standard Q^2 evolution and other possibilities mentioned here.

The EIC would be ideally suited for measurements of F_L . A measurement of F_L requires data at different values of y for the same x and Q^2 . This can be achieved by varying the center-of-mass energy, which will be readily possible at the EIC. In addition, since the EIC will access a kinematic regime *between* that of HERA and of the fixed-target experiments, that extractions of F_L would also be possible by combination with the existing data. Figure 3 shows projected uncertainties for determination of F_L with the EIC. We show what could be learned about F_L by using solely EIC data and varying the collision energy in four settings. This is compared to earlier NMC and projected HERA results, with theory predictions for F_L were taken from [10]. Measurements at the EIC would open the door to precision studies of F_L and of the glue in the proton.

2.2 The Spin Structure of the Nucleon

Few surprises encountered in the exploration of the structure of the nucleon have had a bigger impact than the discovery by the EMC that the quarks and anti-quarks together carry only about a quarter of the nucleon’s spin [11]. To determine how the constituents of the proton, the fundamental quarks, anti-quarks and gluons of QCD, conspire to provide the spin-1/2 of the nucleon, presents the formidable challenge of understanding a complex composite system in nature and has by now developed into a world-wide quest central to nuclear physics. The proton spin sum-rule:

$$\frac{1}{2} = \frac{1}{2}\Delta\Sigma + L_q + \Delta G + L_g$$

states that the proton spin is the sum of the quark and gluon intrinsic spin (ΔG) and orbital angular momentum ($L_{q,g}$) contributions. Here the dependence of each

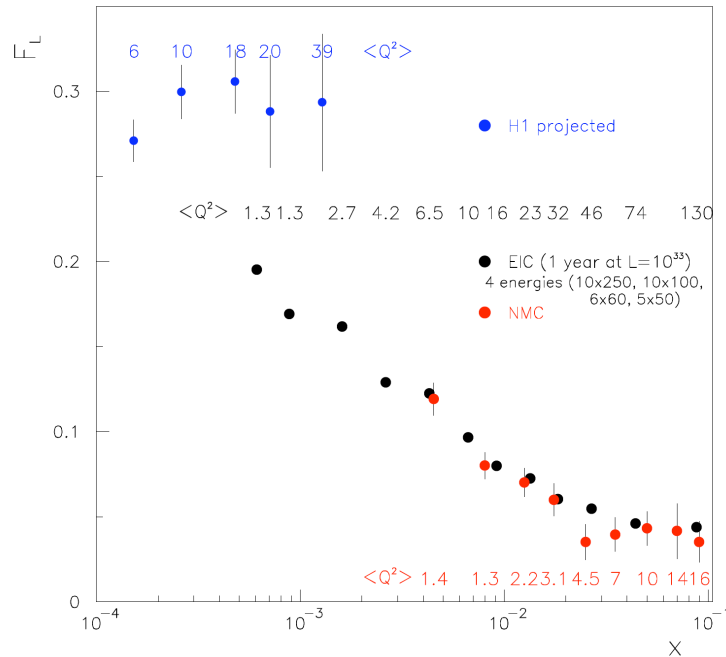


Figure 3. Projected uncertainties for determination of F_L on the proton at EIC from variations of the EIC beam energies.

contribution on the resolution scale Q , which is predicted by QCD, is ignored. EIC with its unique high luminosity, highly polarized electron and nucleon capability, and its extensive range in center-of-mass energy, x and Q^2 , will simultaneously access the quark, sea quark, and gluon contributions through DIS. EIC will build on the results of the important current or forthcoming experiments at CERN [11], DESY [11], RHIC [12], & Jlab [13]. It will extend DIS measurements well beyond the reach of existing accelerators and will provide definitive information on the various contributions to the proton spin, as well as answers to many other questions about spin phenomena in QCD. Scientific highlights and key measurements relating to the spin structure of the proton at EIC are discussed below.

2.2.1 Precision studies of u , d , and s quark & anti-quark polarizations

An important early measurement at EIC would be of the spin-dependent structure function $g_1(x, Q^2)$ of the proton and neutron at values of Bjorken- x down to $\sim 10^{-4}$. This would provide a crucial new verification of the present understanding that the quark and anti-quark spin contribution to the nucleon spin is small. It would make much more reliable the extrapolation of the structure functions to lower x that is needed to extract $\Delta\Sigma$. In addition, it is important to remember that all (fixed-target)

polarized-DIS measurements performed thus far have provided relatively little information on g_1 at $x < 3 \times 10^{-3}$. Where such information is available, Q^2 is usually below the DIS regime, $Q^2 < 1 \text{ GeV}^2$, so that one has to worry about higher-twist contributions that might obscure the extraction of $\Delta\Sigma$. For these reasons, EIC measurements at smaller x than so far possible, and at similar x as before, but with higher Q^2 , should lead to an important consolidation of what we have learned so far, and would dramatically decrease the uncertainty in $\Delta\Sigma$.

As an example, Figure 4 shows projections of the precision expected for the measurement of scaling violations of $g_1(x, Q^2)$ at EIC. We have assumed here collisions of 7 GeV electrons with 150 GeV protons. For comparison we also display the fixed-target g_1 data from SMC, E155, and HERMES[11]. The enormous increase of the kinematic regime in both x and Q^2 that the EIC would offer becomes evident. As we shall discuss shortly, the study of the scaling violations of $g_1(x, Q^2)$ will also allow precise extractions of the proton's spin-dependent gluon distribution.

With precision measurements of $g_1(x, Q^2)$ on the proton and neutron to low x , another scientific highlight at EIC would be a precision test of the Bjorken sum rule [14],

$$\int_0^1 dx [g_1^p - g_1^n](x, Q^2) = 1/6 g_A [1 + O(\alpha_s) + O(1/Q^2)]$$

where g_A is the neutron β -decay constant, and where the schematic terms on the right-hand-side indicate perturbative corrections in the strong coupling α_s and higher-twist contributions, respectively. The Bjorken sum rule is a rare example of a fundamental relationship that is theoretically very well understood within QCD. The perturbative corrections are known through order α_s^3 , and we even have a relatively clear picture about the first higher-twist contributions. Thus, apart from being a remarkable relation between DIS structure functions and a low-energy hadronic quantity, the sum rule also offers unique tests of QCD dynamics, and of our ability to quantitatively describe these. This by itself warrants an experimental study, and it is anticipated that a 2% measurement of the sum rule would be possible at the EIC. At this level, one might actually start to see deviations from the sum rule due to isospin and charge symmetry violations. Relatively little is known about such effects so far, however, so that precision studies of the Bjorken integral also have the potential of providing genuinely new insights.

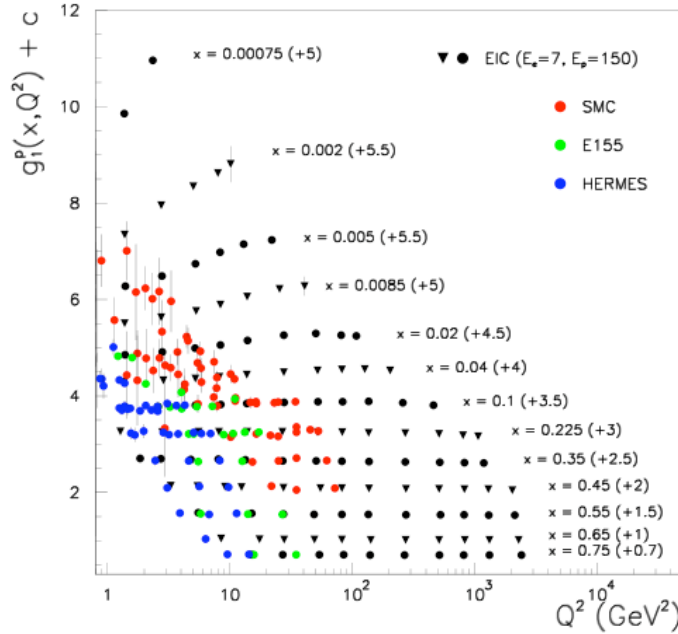


Figure 4. Projected uncertainties for determination of the proton's $g_1(x, Q^2)$ at EIC, assuming collisions of 7 GeV electrons with 150 GeV protons for 5 fb^{-1} luminosity.

Beyond the inclusive g_1 structure function, EIC will provide information with unprecedented detail on the various individual spin-dependent quark and anti-quark densities, Δu , $\Delta \bar{u}$, Δd , $\Delta \bar{d}$, Δs , $\Delta \bar{s}$ in the nucleon. This would give us deeper insight into the question of why the total spin contribution by quarks and anti-quarks is so small. Do the anti-quarks all strongly spin “against” the proton, hereby counteracting the valence contribution and leading to the observed small total quark and anti-quark spin contribution? Or are anti-u quarks positively polarized and anti-d ones negatively, as one might expect on the basis of the Pauli principle? What role do strange quarks play? These, and other questions are also important for comparisons to models of nucleon structure, as well as to lattice calculations that are expected to become extremely powerful and precise on time-scales similar to those of an EIC. A number of fixed-target experiments have performed measurements that are sensitive to the individual polarizations of u,d,s quarks and anti-quarks, but many of the results have remained inconclusive, and important questions have not yet been answered. Crucial information on the Δu , $\Delta \bar{u}$, Δd , $\Delta \bar{d}$ at relatively high momentum fractions x will come from RHIC through its W-physics program, and from the 12-GeV upgrade at Jlab. At the EIC, there are two avenues for very precise measurements of the individual polarizations. One is semi-inclusive DIS (SIDIS), so

far also employed in the fixed-target experiments. By detecting certain hadrons, π^\pm , K^\pm , in final-states in DIS, one may effectively “tag” on the various quark or anti-quark flavors in the proton. Figure 5 shows expectations for the precision with which the spin-dependent quark and anti-quark polarizations would be extracted from SIDIS measurements at EIC.

Further, EIC offers the possibility to carry out measurements of inclusive spin-dependent structure functions in which a W or Z boson, rather than a photon, is exchanged between the electron and the nucleon. Thanks to the nature of the Standard Model couplings, such exchanges violate parity and probe the spin-dependent quark and anti-quark distributions in different combinations than the purely electromagnetic scattering. Measurements of parity-violating structure functions would require the highest possible energies and ideally be performed using electrons as well as positrons. They would lead to probes at moderate to high Bjorken-x that would be complementary to studies in the time-like regime at RHIC, or to the high-x measurements at Jefferson laboratory at much smaller Q^2 .

2.2.2 Precision measurement of spin-dependent gluon distribution at small x

The integral of the spin-dependent gluon distribution over all x,

$$\int_0^1 dx \Delta g(x, Q^2) = \int_0^1 dx [g^\uparrow(x, Q^2) - g^\downarrow(x, Q^2)]$$

gives the gluon spin contribution ΔG to the proton spin. It is the main goal of the spin program at RHIC to perform precise measurements of $\Delta g(x, Q^2)$ over a large range of gluon momentum fractions x, so that the spin contribution ΔG can be obtained from integration over x, assuming an extrapolation to x below (or above) the measured region. HERMES [15, 16] and COMPASS [17] use the photon-gluon fusion process to obtain information on Δg at relatively large x. RHIC is expected to put constraints on Δg all the way down to x of about 10^{-2} from mid-rapidity high- p_T pion, jet, and photon production in running at 200 and 500 GeV center-of-mass energies. Access to somewhat lower x should become possible by performing measurements at very forward angles of the produced final states, where however the

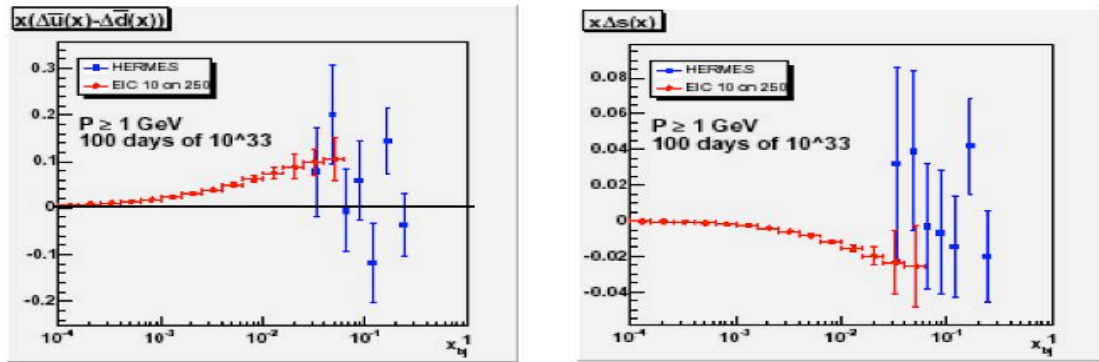


Figure 5. Left: projected precision of EIC measurements of $x(\Delta u - \Delta d)$, compared to the statistical accuracy of the corresponding HERMES measurements [10]. Right: same for $x\Delta s(x)$ from spin-asymmetries for semi-inclusive K^\pm measurements.

underlying theoretical calculation is perhaps slightly more challenging.

Measurements of Δg at x well below 10^{-2} may turn out to be vital for reliably constraining the integral. As an example, a typical currently favored spin-dependent gluon distribution such as the GRSV “standard” one [20], receives more than 30% of its integral from the region $x < 10^{-2}$, at $Q^2 = 10 \text{ GeV}^2$. With EIC, it will be possible to measure $\Delta g(x, Q^2)$ down to x values of a few times 10^{-4} , hereby dramatically reducing the extrapolation uncertainties on the integral. The main tool for performing such measurements would be scaling violations of the spin structure function g_1 . Roughly speaking, the logarithmic derivative of g_1 in Q^2 is at low x proportional to the *negative* of Δg . From this one finds that a large positive gluon distribution drives g_1 at low x to more and more negative values when Q^2 increases, and vice versa. Figure 6 demonstrates this effect, using a variety of spin-dependent parton distributions from the GRSV analysis [20], which mostly differ in the gluon distributions. The blue curve is for a large negative Δg , the green one for a large positive one. The figure also displays projected EIC data, assuming 7 GeV on 150 GeV collisions at $L = 5/\text{fb}$. The great potential of the EIC in providing precise information on $\Delta g(x, Q^2)$ is obvious. See also similar studies in [21].

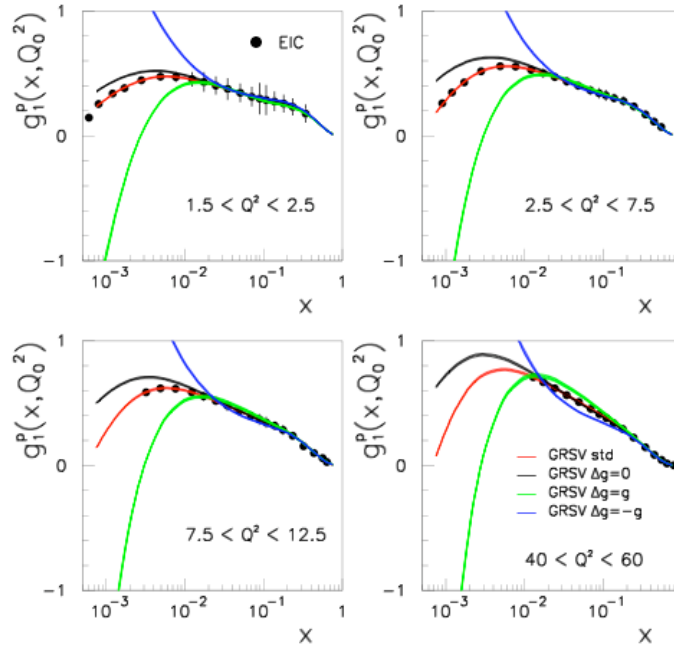


Figure 6. Projected EIC data for the proton structure function $g_1(x, Q^2)$ as a function of x in four Q^2 bins, measured in $150 \text{ GeV} \times 7 \text{ GeV}$ collisions, for 5 fb^{-1} integrated luminosity. Error bars are statistical. The curves show the theoretical predictions based on different sets of spin-dependent parton distribution functions of [20].

Charm production is another channel that could provide precise information on Δg at small to moderate x at an EIC. Figure 7(a) shows projections for the statistical uncertainties on $\Delta g/g$ that would be expected. At higher x , measurements of Δg at the EIC are possible in di-jet production [21], selecting the photon-gluon fusion process. Corresponding projections for the extracted gluon distribution in this case are also shown in Fig. 7(b). We note that the COMPASS and HERMES experiments also make use of the photon-gluon fusion process to constrain Δg . However, at much higher energies, the underlying theoretical interpretation is much cleaner. These measurements at EIC would be complementary to those currently underway at RHIC, which would provide an important test of our understanding of the probes used for measuring Δg .

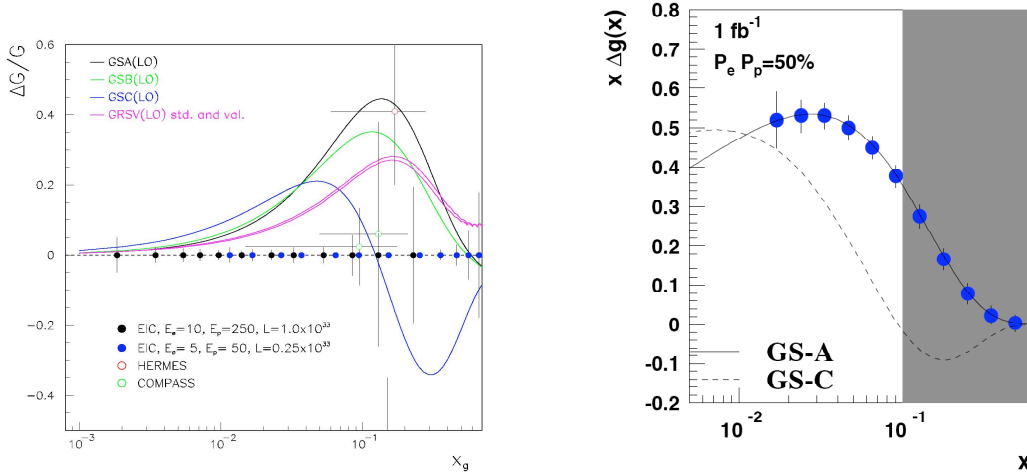


Figure 7. (a) Left: projected uncertainties in the determination of $\Delta g(x)/g(x)$ at EIC using the channel $D^0 \rightarrow K\pi^+$ in charm production. The integrated luminosity is 10 fb^{-1} for the 10 GeV electron on 250 GeV proton measurement, and 2.5 fb^{-1} for 5 GeV electrons on 50 GeV protons. We also show the currently available COMPASS and HERMES data points on $\Delta g(x)/g(x)$ from the photon-gluon fusion process. (b) Right: expected statistical uncertainties of the extracted spin-dependent gluon distribution from measurements of $ep \rightarrow \text{jet jet } X$ at EIC, assuming 1 fb^{-1} luminosity [21].

2.2.3 Generalized Parton Distributions & hard exclusive processes

The structures probed in elastic and inelastic electron scattering - form factors and parton distributions - have traditionally been discussed as separate concepts, with no apparent relation between them. Only recently was it realized that in fact they represent special cases of a more general, much more powerful, way to characterize the structure of the nucleon, the “Generalized Parton Distributions (GPDs)”. The GPDs are the Wigner quantum phase space distribution of quarks in the nucleon - functions describing the simultaneous distribution of particles with respect to both position and momentum in a quantum-mechanical system, representing the closest analogue to a classical phase space density allowed by the uncertainty principle. In addition to the information about the spatial density (form factors) and momentum density (parton distribution), these functions reveal the correlation of the spatial and momentum distributions, *i.e.*, how the spatial shape of the nucleon changes when probing quarks and gluons of different wavelengths.

The concept of GPDs has in many ways revolutionized the way scientists think about the structure of the nucleon. First, it has led to completely new methods of

“spatial imaging” of the nucleon, either in the form of 2-dimensional tomographic images (analogous to CT scans in medical imaging), or in the form of genuine 3-dimensional images (Wigner distributions). Second, GPDs allow us to quantify how the orbital motion of quarks in the nucleon contributes to the nucleon spin - a question of crucial importance for nucleon structure. For a detailed description of the physics of GPDs, see the dedicated White Paper [18].

Measurements of GPDs in hard exclusive processes with an ep/eA collider are much more challenging than traditional inclusive deep-inelastic scattering experiments. In addition to requiring substantially higher luminosities because of small cross sections and the need for differential measurements, the detectors and the interaction region have to be designed to permit full reconstruction of the final state. A properly designed collider would, however, permit exclusive measurements which are very difficult in fixed-target experiments, *e.g.*, processes which require detection of target fragments, such as coherent scattering from nuclei, or exclusive reactions in which the nucleon undergoes a transition to an excited state, $N \rightarrow N^*$.

In assessing the prospects for measurements of exclusive processes in ep scattering at collider energies, $W^2 \gg 10 \text{ GeV}^2$, one needs to distinguish between “diffractive” (no exchange of quantum numbers between the target and the projectile/produced system) and “non-diffractive” processes (exchange of quantum numbers). In diffractive channels, such as J/Ψ , ρ^0 , ϕ production and DVCS (γ production), the cross sections rapidly rise with the collision energy, W . At large Q^2 , these processes probe the gluon GPD and/or the singlet quark GPD. In non-diffractive channels, such as π^{+-} , π^0 , ρ^+ , K production, the cross sections do not rise significantly or perhaps even decrease with energy. These processes at high Q^2 probe the flavor/charge/spin non-singlet quark GPDs describing the quark structure of the target. They require significantly higher luminosities and are generally much more difficult to measure at high energies than the diffractive channels.

Measurements of exclusive reactions in *diffractive* channels with a high-luminosity ep collider would enable a detailed program of transverse gluon and singlet quark imaging of the nucleon, see [19] for a review. J/Ψ electroproduction is a unique probe of the gluon GPD in the proton, whose t -dependence contains the information about the transverse spatial distribution of gluons. Of particular physical interest is

the change of the transverse spatial distribution of gluons with x ; *e.g.*, chiral dynamics predicts that for $x < M_\pi / M_N \sim 0.1$ the nucleon's pion cloud should give rise to a distinctive “Yukawa tail” in the transverse spatial distribution of gluons at large impact parameter b [22]. Measurements of DVCS and exclusive ρ° electroproduction at high Q^2 allow one to probe the singlet quarks in addition to the gluon GPD. Analyzing DVCS and ρ° production together with J/Ψ , which probes the gluon only, one can disentangle the singlet quark and gluon GPDs, and test the evolution of the GPDs predicted by QCD.

As an example of the precision which could be achieved in such measurements, Figure 7 shows projected results for the DVCS differential cross section, $d\sigma/dt$, for several values of x and Q^2 , where t is the momentum transfer on the nucleon line. The integrated luminosities assumed in these simulations correspond to two weeks of running with 100% efficiency. One sees that excellent statistics can be achieved in fully differential measurements in x , Q^2 and t , and over a wide kinematic range, allowing for numerous detailed studies of the reaction mechanism (Q^2 -scaling behavior, QCD evolution) and extraction of information about the nucleon GPDs (transverse distribution of singlet quarks/gluons and its change with x). On the figures, the uncertainties of the assumed x -dependence ($-x^\delta$) and t -dependence ($-e^{-Bt}$) are indicated, and show that reasonable results can already be obtained for a modest beam time. For this program, it will be of great help to have both electron and positron beams at one's disposal, and polarization of both lepton and hadron beams.

Measurements of exclusive meson production in *non-diffractive* channels with a high-luminosity ep collider would allow for detailed studies of the spin-, flavor- and spatial distributions of quarks in the nucleon at $x < 0.1$, complementing the information from DVCS experiments in the valence quark region, $x > 0.1$. A collider could achieve momentum transfers of the order $Q^2 \sim 10 \text{ GeV}^2$, where higher-twist corrections in the GPD analysis are under theoretical control. Much interesting information can already be gained by comparing observables for different meson channels, without detailed modeling of the GPDs. For example, comparison of π° and η provides model-independent information about the ratio of the quark spin distributions Δu and Δd and their spatial distributions. Comparison between π^+ and K^+ production, as well as between ρ^+ and K^{*+} allows one to study SU(3) flavor

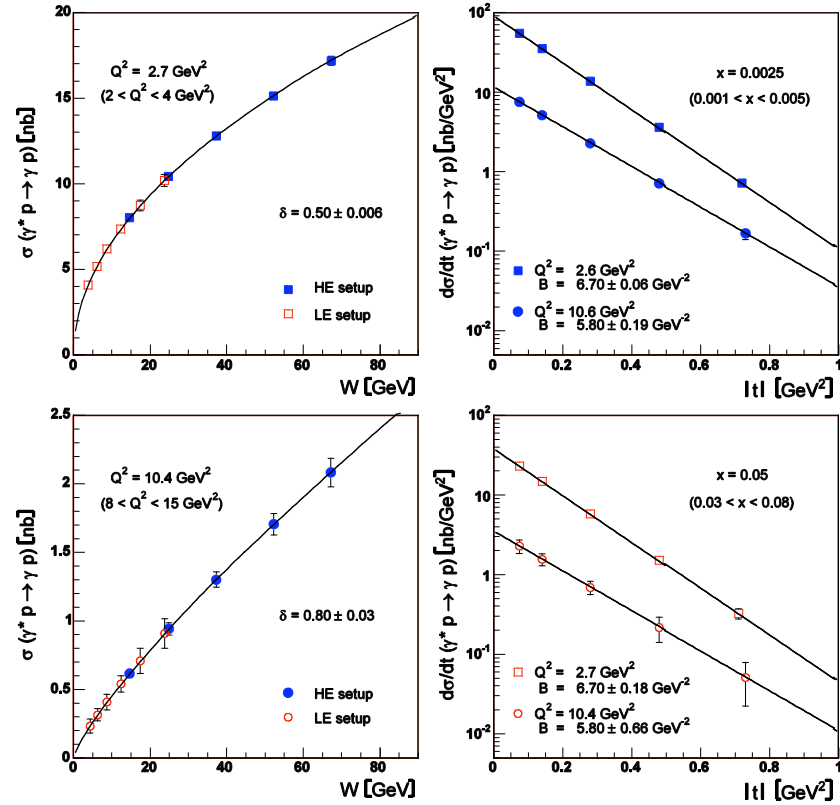


Figure 8. (a) Left panel: projected results for the total DVCS cross section with an EIC, as a function of W for two values of Q^2 . (b) Right panel: differential cross section $d\sigma/dt$ for two representative values of x and Q^2 . The projections assume a high-energy setup (10 on 250 GeV), with an integrated luminosity of 530 pb^{-1} for the smaller x -value, and a low-energy setup (5 on 50 GeV) with 180 pb^{-1} for the larger x -value. The estimates of the event rates here assume 100% detector acceptance.

symmetry breaking in the nucleon's quark distributions in different spin/parity channels, and in the meson wave functions.

2.2.4 Transverse Spin & Transverse-Momentum Dependent Parton Distributions

Azimuthal distributions of final state hadrons in semi-inclusive deep inelastic scattering provide an independent window on the orbital motion of quarks, through the framework of Transverse-Momentum Dependent Parton Distributions (TMDs). TMDs were in particular considered for explaining the surprisingly large single-transverse spin asymmetries found in hadronic reactions and in semi-inclusive deep inelastic scattering experiments at HERMES, COMPASS, and JLab. Recent theoretical work has established a framework that provides a rigorous basis for

extracting TMDs from the great wealth of existing and future semi-inclusive deep inelastic scattering data for different spin-dependent and spin-independent observables.

The so-called “Sivers” function expresses the correlation between the transverse momentum of a parton, ejected from a transversely polarized nucleon, and the momentum and transverse spin of that nucleon. The function requires both orbital angular momentum as well as a non-trivial phase, which may arise from a rescattering of the struck parton in the color field of the nucleon remnant. The Sivers functions therefore probe the color Lorentz forces exerted by the nucleon remnant on a struck parton. To date, initial crude experimental results on this Sivers function are consistent with a heuristic model of up and down quarks orbiting the nucleon in opposite directions, consistent with their contributions to the nucleon’s magnetic moment. Measurements at an EIC would allow precision studies of the TMDs, including their dependence on transverse momentum. Furthermore, they would definitively clarify if the associated azimuthal asymmetries in semi-inclusive DIS are indeed leading-twist effects, through studies of their Q^2 dependence. Figure 9 shows the expected statistical accuracies with which measurements of Sivers-type spin asymmetries would be measured at an EIC.

The “Boer-Mulders” function describes the correlation between the transverse spin and momentum of a quark in an unpolarized target. It is thus similar to the Sivers function except that the quark spin instead of the nucleon spin is relevant. The simplest mechanism that can lead to a non-zero value of this function is a correlation between the spin of the quarks and its orbital angular momentum.

Related spin effects in the fragmentation process, expressed by so-called “Collins” functions, allow new insights into hadronization (see below), and may serve as a tool to obtain precise measurements of the transversity distributions of quarks and anti-quarks in the proton. In the non-relativistic quark model, the transversity distributions are equal to their helicity counterparts discussed earlier, hence, any difference probes relativistic effects in nucleon structure. The integral of the transversity distributions for quarks minus anti-quarks is one of the fundamental charges of the proton, its tensor charge. We note that information on the Collins functions is now becoming available from measurements in e^+e^- annihilation at BELLE.

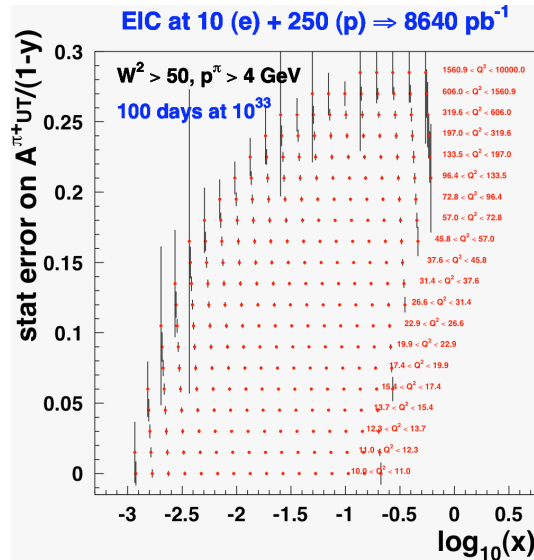


Figure 9. Expected statistical accuracies for the Sivers-type azimuthal asymmetry $A_{UU}^{\cos 2\phi}$ in semi-inclusive pion production at the EIC, as a function of x for various fixed Q^2 s.

2.2.5 Studies of Hadronization

The formation of confined hadronic final-states from the quarks and gluons produced in a perturbative hard-scattering is clearly one of the most profound phenomena in QCD, but is so far little understood. Precision studies of kinematic distributions and properties of the hadronic final states in DIS at an EIC will provide valuable new information. As an example, studying the Collins function described above, will show what role quark motion and spin play. The collider geometry will in particular allow measurement of all reaction products, with a dramatic increase in our knowledge of the essentially unknown target-fragmentation region. This can, *e.g.*, be used to study how, and to what extent, the spin of a quark is transferred to its hadronic daughters.

2.2.6 Spin structure of the photon

EIC will also provide the first measurement of the spin-dependent structure functions of the photon, possible by studying spin asymmetries in photo-production reactions [27]. These might offer unique insights into the spin structure of vector mesons like the ρ , which are not attainable in any other way we know of. An exciting question that one might possibly be able to address would be: does the ρ show a similar “spin crisis” as the nucleon?

2.3 What are the properties of high-density partonic matter?

Our current understanding of hadron structure indicates that the proton is overwhelmingly comprised of gluons for $x \leq 0.01$. In nuclei, the regime of $x < 0.01$ is *terra incognita*. EIC offers the unprecedented opportunity to map the fundamental structure of nuclei in this glue dominated kinematic region.

Simple arguments in QCD suggest that, at small x , the field strengths of gluon fields should be the maximum possible in nature, corresponding to a novel non-linear regime of the theory. The physics governing gluon interactions in this regime may be universal across hadrons and nuclei.

Further simple arguments indicate that this non-linear regime is reached at larger values of x in heavy nuclei and its effects amplified by nuclear size. Studies of the properties of gluons and the accompanying sea quarks in this regime, across a wide range of nuclei, have the potential to fundamentally impact our understanding of QCD at high energies.

The possible impact of such studies can be better appreciated in the context of what we know. At larger x , and at large momentum transfers Q , the properties of quarks and gluons are well described by the linear evolution equations of perturbative QCD (pQCD). These predict, for fixed Q and decreasing x , the density of gluons grows by hard (large x) partons successively shedding softer partons in a self-similar cascade. This bremsstrahlung picture is well confirmed in a wide kinematic range by the HERA experiments. However, at smaller x , when the density of gluons from the cascade becomes large, multi-gluon correlations appear causing softer gluons to recombine into harder ones. When these correlations become large, strong deviations from linear evolution must occur. Gluon saturation is a simple mechanism for nature to prevent the rapid growth of gluons from violating the “black disk” limit set by the unitarity of the theory.

What are the properties of QCD in this novel regime of gluon saturation? Theoretical predictions suggest that the properties of this saturated gluonic phase are controlled by a dynamical saturation scale $Q_s(x,A)$, which grows as x gets smaller and the nuclear size A gets larger. When this scale is much larger than the fundamental scale of the theory (~ 200 MeV), asymptotic freedom predicts that the

QCD coupling constant in the gluon saturation regime is weak, thereby making systematic computations feasible. These suggest that the properties of saturated gluons may be described as a Color Glass Condensate (CGC) [26]. Data from HERA at small x and RHIC in forward (small x) kinematics are consistent with saturation models albeit not conclusively so. Alternative candidates for the appropriate degrees of freedom in QCD at high energies are color neutral excitations with vacuum quantum numbers called Pomerons; these come in soft (non-perturbative) or hard (perturbative) varieties.

The properties of gluons in nuclear wavefunctions are vital to better understand the formation and thermalization of hot and dense gluonic matter produced when nuclei are smashed together at the high energies of RHIC and the future LHC collider. Initial conditions for hydrodynamic flow and bulk properties of RHIC's perfect fluid are sensitive to the centrality and energy dependence of the saturation scale Q_s . Further, high energy cross-sections for hard processes are proportional to the product of the nuclear gluon distributions in the colliding nuclei. In Fig. 8b, model predictions differ by a factor of 3 for the nuclear gluon distributions at LHC energies: this corresponds to an order of magnitude range in cross-sections for semi-hard final states at the LHC.

How can we explore the glue dominated regime of nuclei with EIC? We can do so by addressing the following questions:

- What is the momentum distribution of gluons (and sea quarks) in nuclei?
- What is the space-time distribution of gluons (and sea quarks) in nuclei?
- How do fast probes interact with an extended gluonic medium?
- Do strong gluon fields enhance the role of color neutral (Pomeron) degrees of freedom in scattering off nuclei?

We shall now briefly discuss measurements with EIC that will address these questions. A more detailed discussion can be found in the EIC position paper on eA collisions [29].

2.3.1 Momentum distributions of gluons and quarks in nuclei:

The x and Q^2 distributions of gluons and quarks in nuclei are extracted through the following channels.

i) *Structure function measurements:* The fully inclusive structure functions F_2 and F_L offer the most precise determination of parton (quark and gluon) distributions in

nuclei as discussed in the section Scientific Highlights (page 8). The former is sensitive to quark distributions; the latter to gluon distributions. Scaling violations of F_2 with Q^2 are also sensitive to gluon distributions. In Fig. 8a, we show projections from pQCD based models with differing amounts of shadowing and from a saturation (CGC) model for the normalized ratio of structure function compared to the statistical precision expected with 0.02 nucleus fb^{-1} of data for 10 GeV electrons on 100 GeV gold nuclei. Fig. 10a suggests that data can distinguish between differing model predictions. In Fig. 10b, the ratio of gluon distributions extracted from the longitudinal structure is shown for 10 nucleon fb^{-1} data for DIS on lead nuclei. At small x , to good approximation, $F_L^A / F_L^D \sim G_A / G_D$. Measurements of the charm structure functions F_2^C and F_L^C provide first data on nuclear charm quarks distributions at $x < 0.1$ - the high luminosities of EIC give estimates of 10^5 charm pairs for 5 fb^{-1} enabling precision charm studies [29]. Measurements of nuclear gluon distributions in the kinematic region around $x=0.1$ either through charm or scaling violations will allow one to pin down gluon anti-shadowing which is critical to a microscopic understanding of nuclear binding. Measurements at $x > 0.3$ are sensitive to the intrinsic charm component in nuclei which dominates conventional (photon-gluon fusion) charm production mechanisms in this kinematic regime [30].

ii) *Semi-inclusive final states*: Photon-gluon fusion results in semi-inclusive final states that are sensitive to the nuclear gluon distributions. Noteworthy examples are di-jets channels. In the latter case, the QCD Compton process also contributes-for further discussion in the context of eA studies, see [31].

iii) *Exclusive final states*: Measurements of elastic vector meson production $eA \rightarrow (\rho, \varphi, J/\psi)A$ are extremely sensitive to the nuclear gluon density. The ratio of forward cross-sections in pQCD, for longitudinally polarized photons, is proportional to the ratio of gluon distributions *squared* [32] -the Q^2 dependence changes significantly in the non-linear regime from $1/Q^6$ to $1/Q^2$ [33].

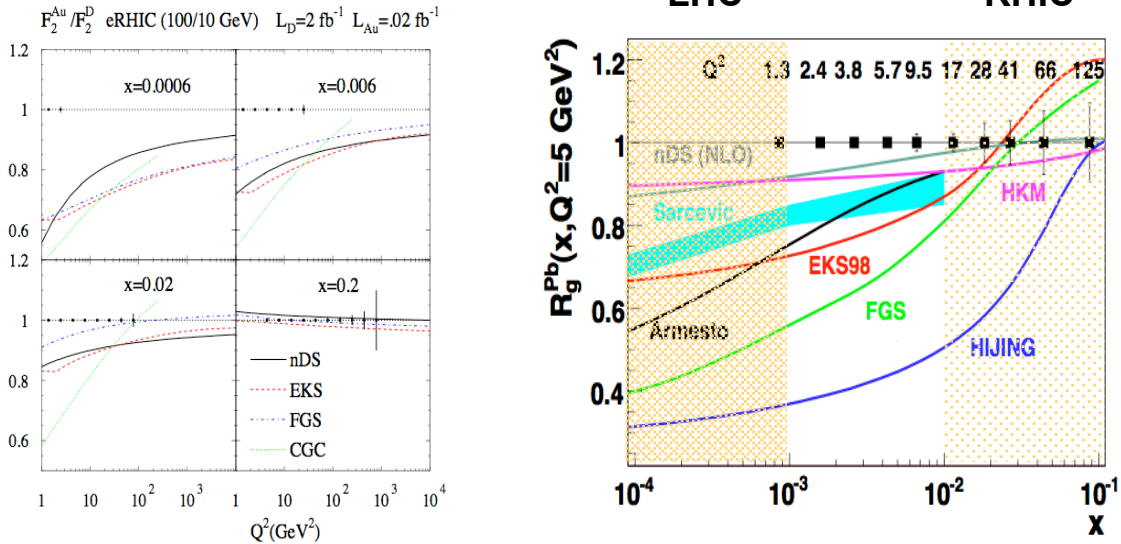


Figure 10.a) LEFT: Statistical uncertainties of the ratio of F_2 (representing the sum of the quark and anti-quark distributions) in gold nuclei to deuterium. b)RIGHT: The ratio of gluon distributions in lead relative to deuterium. $L_p = 10 \text{ fb}^{-1}$ is assumed in 8b. In 8a, nDS, EKS and FGS represent pQCD models with different shadowing; CGC is a saturation model prediction. In 8b, additional shadowing parametrizations are shown. Shaded region in 8b is the kinematic domain for semi-hard processes in AA collisions at the LHC.

2.3.2 Space-time distribution of gluons and quarks:

In DIS, at small x , the virtual photon fluctuates into a quark anti-quark dipole which scatters coherently on the hadron or nucleus. Combined use of the dipole model for total cross-sections and differential cross-section for the elastic production of vector mesons enables one to estimate the differential cross-section for the dipole to scatter elastically.

The Fourier transform of the vector meson cross-section, as a function of the momentum transfer t along the proton line allows one to estimate the S-matrix for this amplitude. The optical theorem is then employed to extract the survival probability of small sized dipoles of size d to propagate through the target at a given b without interacting. In pQCD, this probability is close to 1. This should be contrasted with the survival probability in fig. 11 extracted from dipole models. The Munier et al. [34] curves correspond to results from the elastic production of ρ^0 mesons.

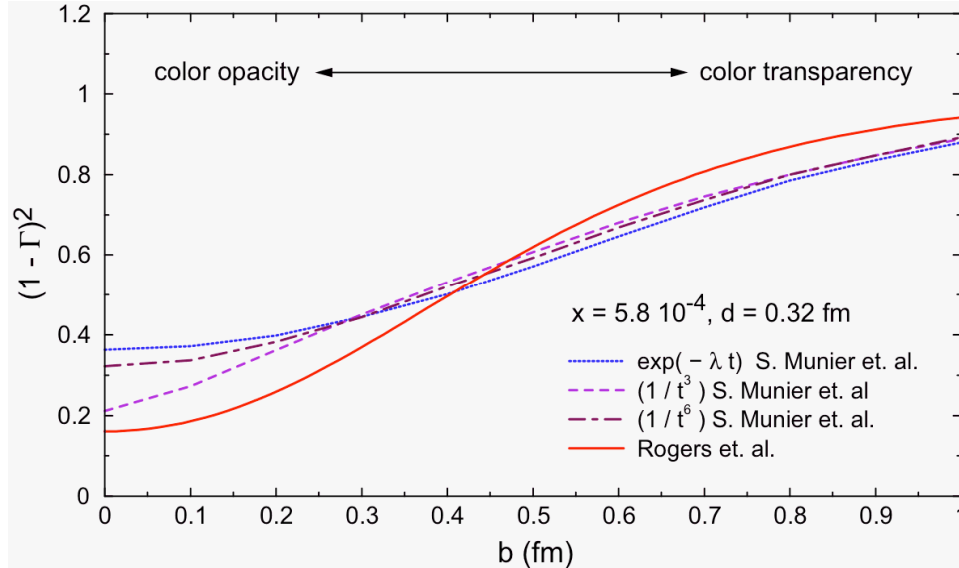


Figure 11. Survival probability versus impact parameter b of a quark-antiquark pair of size $d=0.32$ fm scattering off a proton extracted from HERA data on elastic production of vector mesons[34].

HERA data for this process are limited and the curves result from differing extrapolations. The Rogers et al. [35] curve uses data on elastic J/ψ production allowing reliable extrapolation to lower impact parameters; the agreement at large b of these models is within 5%. At $b=0$, the survival probability of dipoles can be as low as 20% suggesting very strong gluon fields localized at the center of the proton. A systematic dilution of the interaction strength (*color transparency*) is seen for larger b . Similar analyses for large nuclei give the survival probability of small sized (0.3 fm) dipoles from 60% at $x=0.01$ to as low as 10% at $x=0.001$ [35].

Estimates of the quark saturation scale give $Q_s^2(\text{proton}) \sim 0.6 \text{ GeV}^2$ at $b=0$ and $x=10^{-4}$ [36]. Because strong gluon fields dilute rapidly with b in the proton, the effective saturation scale for most processes is significantly smaller making saturation effects harder to isolate. In contrast, the b profile of nuclei is more uniform. In Fig. 12, we show the estimated [36] saturation scale for gold and calcium nuclei at $b=0$ as a function of x relative to the median saturation scale in the proton. The nuclear enhancement is quite significant. Therefore, in large nuclei at small x , EIC will uniquely and cleanly access a regime of semi-hard $Q_s > Q$. In this kinematic region, the running of the QCD coupling constant will be determined by Q_s ; this suggests that precision weak coupling QCD calculations can be compared to data in this novel strong gluon field regime.

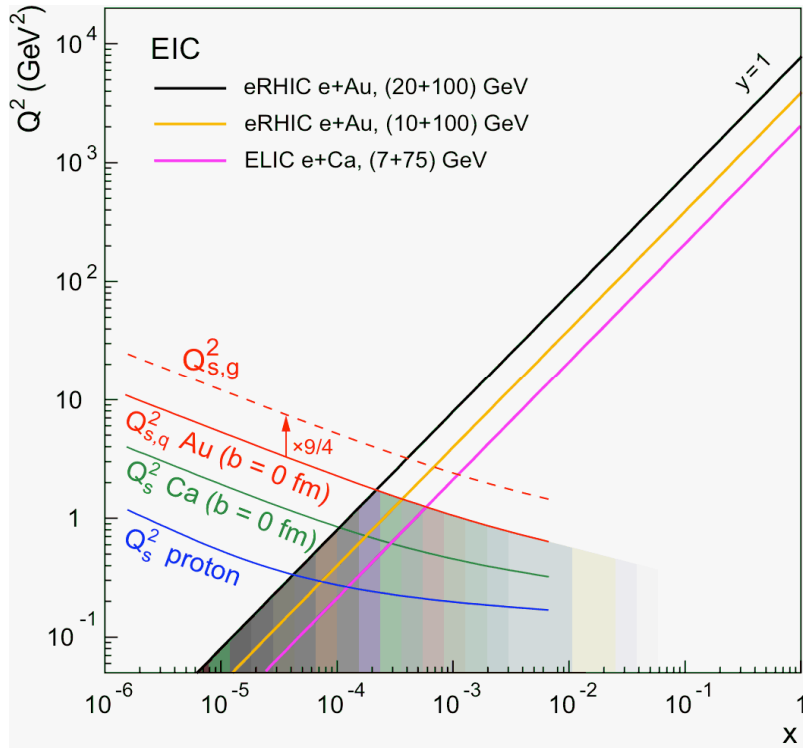


Figure 12. The quark saturation scales in gold and calcium at $b=0$ and the median quark saturation scale in the proton are shown superposed on the kinematic EIC x - Q^2 acceptance. The gluon saturation scale is larger than the quark saturation scale by the color factor $9/4$.

Deeply Virtual Compton Scattering (DVCS) studies, discussed previously, also provide insight into the space-time structure of nuclei, particularly for $x > 0.1$. Independent motivation for such studies comes from preliminary RHIC data from PHENIX showing suppression of direct photons in central Au-Au collisions at large p_T .

2.3.3 Scattering and hadronization of fast probes in an extended gluonic medium:

The previous discussion pertains to small x where the probe interacts coherently with the entire nucleus and strong gluon field effects are enhanced by nuclear size. At larger x , the probe is coherent over only part of the extended nuclear medium. Ratios of inclusive hadron distributions in nucleons and nuclei measure nuclear effects as a function of photon and hadron kinematics. The large energy span of EIC enables extensive studies [37] of the nature of parton energy loss and in medium fragmentation with collider kinematics. *Novel measurements are the attenuation of charm*

and bottom quarks and the in-medium formation of D and B mesons. Such studies are especially compelling because recent RHIC results indicate that charm and likely bottom quarks are quenched in hot matter more than anticipated by radiative energy loss models.

2.3.4 Role of color neutral degrees (Pomeron) of freedom in scattering off nuclei:

Diffraction interactions result when the lepton probe interacts with a color neutral vacuum excitation, which may be visualized as colorless combination of two or more gluons in the hadron or nucleus. At HERA, an unexpected discovery was that ~15% of the ep cross-section is from diffractive final states—a striking result implying the proton at rest remains intact one seventh of the time when struck by a 25 TeV electron. Several saturation/CGC models of strong gluon fields in nuclei suggest that large nuclei are intact nearly 40% of the time—nearly saturating the quantum mechanical black disc limit of 50%. For a recent study, see [38]. Very significantly, even though the nuclei are intact, the diffractively produced final states are semi-hard with momenta $\sim Q_s^A$. Multi-gluon interactions are enhanced in large nuclei—can these be described in terms of universal quasi-particle degrees of freedom? Measurements of coherent diffractive scattering on nuclei are easier in the collider environment of EIC relative to fixed target experiments. They will provide definitive tests of strong gluon field dynamics in QCD. Preliminary studies indicate that such measurements are not statistics limited but will be strongly influenced by detector issues.

2.3.5 Complementarity of pA and eA studies at small x:

Forward deuteron-nucleus scattering at RHIC shows strong shadowing of inclusive pion distributions at small x in nuclei. These are consistent with CGC predictions; albeit, other model explanations are not ruled out. Future deuteron-gold (proton-lead) measurements at RHIC (LHC) widely extend the scope of these studies and have significant discovery potential.

They will be complementary to measurements at EIC. Precision measurements of the gluon distribution will be more challenging at a hadron collider. The fundamental physics questions driving complementary studies of pA and eA are about the universality of observables extracted with the respective hadronic and leptonic probes. Factorization theorems predicated on universality are proven only for a small

class of inclusive observables. They fail dramatically for ep and pp diffractive final states [39]. Factorization is uncertain in the strong gluon field regime even for inclusive observables [40]. Unambiguous extraction of the properties of a novel strong field regime of QCD requires complementary probes.

3 The Electron Ion Collider: Realization

Since the 2001 Long Range Plan, there has been significant progress in the design of both the EIC accelerator and the detectors required to carry out the experiments.

3.1 EIC Accelerator Design

There are two complementary concepts to realize EIC:

- to construct an electron beam (either ring or linac) to collide with the existing RHIC ion complex. This is known as eRHIC
- to construct an ion complex to collide with the upgraded CEBAF accelerator. This is known as Electron-Light-Ion-Collider or ELIC.

eRHIC

One of the early EIC accelerator design effort focused on utilization of the existing RHIC ion complex and is summarized in a comprehensive document, the Zero Order Design Report (ZDR) [41] which has been reviewed by the RHIC Machine Advisory Committee. The existing RHIC complex allows polarized protons to be stored for collisions from 30 to 250 GeV/c. The soon to be installed EBIS source will allow all nuclei up to Uranium to be accelerated to 100 GeV/c per nucleon. The ZDR contains two possible ways to realize eRHIC:

- an eRHIC ring-ring (RR) design, which involves construction of an electron ring complex along side the RHIC and have polarized 10 GeV/c electrons or positrons collide with RHIC beams
- an eRHIC LINAC-ring design, which involves construction of a 10 energy recovery linac (ERL)

Both designs assume certain changes are made to the RHIC rings, for example, increasing the number of proton bunches from 120 (up to 111 filled) to 180 (up to 166 filled). This will need some dedicated R&D effort in the near future [41].

The RR design meets the basic scientific specifications as layed out in the 2002 NSAC White Paper on EIC[5] for all the inclusive and most of the semi-inclusive DIS measurements. It utilizes existing accelerator technology and can achieve

average luminosity¹ of $\sim 2 \times 10^{32}$ /cm²/s. With some extrapolation beyond demonstrated capabilities, and further R&D effort on the hadron beams, a luminosity close to 10^{33} /cm²/s may be possible. The cost of the eRHIC ring-ring design has been estimated with some detailed considerations and is the basis for planning by both BNL and DOE.

The ZDR also describes another concept of eRHIC to realize significantly higher average luminosities of a few times 10^{33} /cm²/s with eRHIC using an energy-recovery linac. The linac-ring design shows further promise due the potential simplicity of the IR design, ease and transparency of polarization through a range of electron beam energies [41]. The high intensity polarized electron current source and the energy recovery capability require extensive R&D effort. Positron beam could be realized with the addition of a storage ring. Having finalized the ring-ring design, and understood its conceptual limits, this linac-ring version of eRHIC is now the focus of eRHIC accelerator group.

Electron Light Ion Collider (ELIC) at Jefferson National Laboratory

Accelerator physicists at Jefferson Lab are pursuing an Electron-Light Ion Collider, ELIC, which uses the CEBAF linear accelerator and requires the construction of a 30 to 225 GeV ion storage ring in its vicinity. This represents an ambitious design concept to realize peak luminosities of up to few $\times 10^{34}$ /cm²/s, using much higher collision frequencies and crab-crossing of colliding beams. A detailed summary of this design effort, and associated R&D requirements, is given in the ELIC ZDR [42]. In this concept, the booster rings, electron collider ring, and ion collider ring are designed as a “figure 8”, a design directly aimed at spin physics opportunities. This ring-ring design could be substituted by a linac-ring design using CEBAF as a one-pass energy recovering linac, should future R&D warrant this. While polarized beams of proton, deuteron and helium (³He) are possible, beams of nuclei up to Calcium are included in the baseline design. Heavy nuclei up to Lead are possible without significant change. Four interaction regions for detectors are possible in the present design.

¹ Peak luminosity is about three times larger.

3.2 EIC Detector Design

EIC detector design will naturally use the experience of operating the H1 and ZEUS detectors at DESY. Further, it will be optimized for the physics that could not be pursued at DESY due to the limitations of those detectors. In view of the different physics objectives, EIC must have detection of full hadron final states incorporated into the detector design. To optimally benefit from the higher luminosity, the detector design will have to be integrated with the machine and interaction region design.

The following requirements constitute the minimal capabilities of a future EIC detector:

- Measurement of the energy and angle of the scattered electron (kinematics of the DIS reaction)
- Measurement of the hadronic final state (kinematics of DIS reaction, jet studies, flavor tagging, fragmentation studies, precision vertex detection and particle ID system for heavy flavor physics, and K/ π separation)
- Close to full 4π -detector acceptance and high enough precision of the above, to allow precise determination of missing transverse energy (Events involving neutrinos in the final state, electro-weak physics)

In addition to these demands on a central detector, the following forward and rear detector systems are crucial:

- Zero-degree photon detector to control radiative corrections and measure Bremsstrahlung photons for luminosity measurements (absolute and relative with respect to different ep spin combinations)
- Tag electrons under small angles (<1) to study the non-perturbative and perturbative QCD transition region
- Tagging of forward particles (Diffraction and nuclear fragments)

Optimizing all of the above requirements is a challenging task. Two detector concepts have been considered so far: One, which focuses on the rear/forward directions and thus on low-x / high-x physics, which emerges out of the HERA-III detector studies [43]. This detector concept is based on a compact system of tracking and central electromagnetic calorimetry inside a dipole magnetic field with calorimetric end-walls. Charged particles produced in the forward direction are bent

into the detector volume, which extends the rapidity coverage compared to existing detectors.

The second design effort [44] focuses on a wide acceptance detector system similar to the current HERA collider experiments H1 and ZEUS to allow for the maximum Q^2 range possible. The physics program to be pursued with this detector will demand high luminosity. This will drive the close proximity of focusing beam elements and will have to be balanced by the need to preserve good detector acceptance. The hermetic inner and outer tracking system including the electromagnetic section of a barrel calorimeter will be surrounded by an axial magnetic field. The forward calorimeter will be subdivided into hadronic and electromagnetic sections. Detector MC studies are being performed with different physics processes of interest to refine and identify detector R&D needs.

3 Conclusion

The concepts and the machine parameters for the EIC have evolved over a decade from workshops and meetings within the international nuclear physics community. EIC is the next generation QCD machine in the U.S. beyond the present JLab and RHIC programs. The scientific focus is to explore the glue and sea quarks, the main contributors to the mass of the visible universe. A sound accelerator design, which can reach a luminosity of $\sim 10^{32}$ /cm²/sec, is in place and concepts which have the promise of significantly increased luminosity are being developed. EIC will be unique in its physics program and will maintain U.S. leadership in the field of nuclear physics in general and QCD in particular. It will complement the planned facilities in Europe and Asia. There is an existing core support, which is growing robustly as is evidenced by the collaboration list included early in this document. With existing high-energy lepton scattering programs either terminated or scheduled for phase-out in the near future, it is essential that EIC be placed on a trajectory such that realization can get underway by 2012.

References

- [1] Report of the NSAC Subcommittee on Implementation of the 2002 Long Range Plan: http://www.sc.doe.gov/np/nsac/docs/nsac-report-final_Tribble.pdf.
- [2] Proceedings of the Workshop on Physics with a High Luminosity Polarized Electron Ion Collider (EPIC99), April 8-11, 1999, Bloomington, Indiana, USA, Editors: L.C. Bland, J.T. Londergan, and A.P. Szczepaniak, World Scientific.
- [3] Proceedings of the eRHIC Workshop at Yale, Ed. V. W. Hughes and A. Deshpande, BNL-Report-52592
- [4] Proceedings of the Second Workshop on Physics with an Electron Polarized Light Ion Collider (EPIC 2000), September 14-16, 2000, MIT, Cambridge, USA, Editor R.G. Milner, AIP Conference Proceedings No. 588.
- [5] The Electron Ion Collider: A high luminosity probe of the partonic substructure of nucleons and nuclei, February 2002, BNL-Report 68933, Editors: A. Deshpande and R. Venugopalan.
- [6] Abhay Deshpande, Richard Milner, Raju Venugopalan and Werner Vogelsang, *Ann. Rev. Nucl. and Part. Sci.* 55, 2005.
- [7] S. Chekanov et al. [ZEUS Collaboration], *Phys. Rev. D* 67 (2003) 012007.
- [8] L. Lipatov, *Sov. J. Nucl. Phys.* 23:338-345, 1976; E. A. Kuraev, L. N. Lipatov, V. S. Fadin, *Sov. Phys. JETP* 44:443-450, 1976; E. A. Kuraev, L.N.Lipatov, V.S.Fadin, *Sov. Phys. JETP* 45:199-204, 1977; I.I.Balitsky, L. N. Lipatov, *Sov. J. Nucl. Phys.* 28:822-829, 1978.
- [9] E. Iancu and R. Venugopalan, *The color glass condensate and high energy scattering in QCD*, hep-ph/0303204
- [10] C.D. White and R.S. Thorne, *Phys. Rev. D* 75 (2007) 034005
- [11] E.W. Hughes and R. Voss, *Ann. Rev. Nucl. Part. Sci.* 49, 303 (1999); S. Bass, *Rev. Mod. Phys.* 77, 1257 (2005).
- [12] C. Aidala et al., "Research Plan for Spin Physics at RHIC", <http://spin.riken.bnl.gov/rsc/report/masterspin.pdf>.
- [13] The Science and Experimental Equipment for the 12 GeV upgrade of CEBAF, Editors J. Arrington et al., <http://www.physics.rutgers.edu/np/2007lrp-home.html>
- [14] J.D. Bjorken, *Phys. Rev.* 148, 1467 (1966); *Phys. Rev. D* 1, 1376 (1970).
- [15] A. Airapetian et al. [HERMES Collaboration], *Phys. Rev. D* 71, 012003 (2005).
- [16] A. Airapetian et al. [HERMES Collaboration], *Phys. Rev. Lett.* 84, 2584 (2000).
- [17] E.A. Ageev et al. [COMPASS Collaboration], *Phys. Lett.* B633, 25 (2006).
- [18] H. Abramowicz et al, "Exploring the 3D quark & gluon structure of the proton: Electron scattering with present & future facilities" <http://www.physics.rutgers.edu/np/gpdwp.pdf>
- [19] L. Frankfurt, M. Strikman and C. Weiss, *Ann. Rev. Nucl. Part. Sci.* 55 (2005) 403.
- [20] M. Glück, E. Reya, M. Stratmann, W. Vogelsang, *Phys. Rev. D* 63, 094005 (2001).

- [21] G. Raedel, A. De Reock, Nucl. Phys. B (Proc. Suppl.) 105 (2002) 90-94, Editors: S. D. Bass, A. De Roeck, A. Deshpande; A. De Reock, et al., Eur. Phys. J. C6 (1999) 131-145
- [22] M. Strikman and C. Weiss, Phys. Rev. D 69, 054012 (2004).
- [23] X. Ji, Phys. Rev. Lett. 78, 610 (1997).
- [24] M. Burkardt, Int. J. Mod. Phys. A18, 173 (2003).
- [25] X. Ji, Phys. Rev. Lett. 91, 062001 (2003); A.V. Belitsky, X. Ji, F. Yuan, Phys. Rev. D69, 074014 (2004).
- [26] A. Airapetian et al. [HERMES Collaboration], Phys. Rev. Lett. 94, 012002, 2005.
- [27] M. Stratmann, W. Vogelsang, Z. Phys. C74, 641 (1997).
- [28] E. Iancu and R. Venugopalan, hep-ph/0303204; H. Weigert, hep-ph/0501087.
- [29] "Physics Opportunities with an e+A collisions at an electron ion collider", The EIC Collaboration, unpublished, available at: <http://www.bnl.gov/eic>
- [30] B. W. Harris, J. Smith and R. Vogt, Nucl. Phys. B461: 181 (1996).
- [31] Nuclear beams at HERA, M. Arneodo et al., hep-ph/9610423.
- [32] S. Brodsky et al., Phys. Rev. D50: 3134 (1994).
- [33] L. Frankfurt, V. Guzey, M. McDermott and M. Strikman, Phys. Rev. Lett. 87:192301 (2001).
- [34] S. Munier, A. M. Stasto and A. H. Mueller, Nucl. Phys. B603: 427 (2001).
- [35] T. Rogers, V. Guzey, M. Strikman and X. Zu, Phys. Rev. D69: 074011 (2004).
- [36] H. Kowalski and D. Teaney, Phys. Rev. D68:1140505 (2003).
- [37] B. Z. Kopeliovich et al. Nucl. Phys. A740: 211 (2004); A. Accardi, nucl-th/0510090.
- [38] M. S. Kugeratski, V. P. Goncalves and F. S. Navarra, Eur. Phys. J C46: 413 (2006).
- [39] L. Alvero, J. C. Collins, J. Terron and J.J. Whitmore, Phys. Rev. D59: 074022 (1999).
- [40] J. W. Qiu and G. Sterman, Nucl. Phys. B353, 137 (1991).
- [41] eRHIC ZDR, 2004, Ed: M. Farkhondeh & V. Ptitsyn; eRHIC Accelerator Position Paper for NSAC LRP 2007; eRHIC Accelerator Position Paper, prepared for NSAC 2007 Long Range Planning, J. Beebe-Wang et al., <http://www.physics.rutgers.edu/2007/nplrp-2007.html>
- [42] Zeroth-Order Design Report on Electron-Light Ion Collider at CEBAF, January 2007, edited by Ya. Derbenev, L. Merminga and Y. Zhang.
- [43] I. Abt, A. Caldwell, X. Liu and J. Sutiak, hep-ex/0407053.
- [44] B. Surrow, at the XIV International Workshop on Deep-Inelastic Scattering (DIS2006), Tsukuba, Japan, April 2007, hep-physics/0608290.